# *Supplementary Material for*

# Integrative analysis of identifying methylation-driven genes signature predicts prognosis in colorectal carcinoma

## 1 List of Supplementary Material

### Ⅰ Supplementary Figures

Supplementary Figure S1: Flowchart of the research.

Supplementary Figure S2: Correlation between DNA methylation and gene expression of *ANXA9*, *BATF*, *RBP1*, and *SERPINA1* in the training dataset and validation dataset.

Supplementary Figure S3: The difference of expression levels of four methylation-driven genes between tumor tissue and normal tissue.

Supplementary Figure S4: Validation of four-gene risk score model in the GEO dataset.

Supplementary Figure S5: Kaplan–Meier and ROC analyses of CRC patients based on different age, gender, and TNM staging subgroups in the training set.

Supplementary Figure S6: Kaplan–Meier and ROC analyses of CRC patients based on different age, gender, and TNM staging subgroups in the testing set.

Supplementary Figure S7: Comparison of ROC curves between the signature and other known biomarkers in predicting 8-year OS of CRC patients.

Supplementary Figure S8: Gene set enrichment analysis of candidate four methylation-driven genes.

### Ⅱ Supplementary Tables

Supplementary Table S1: 143 epigenetic drivers were identified by MethylMix.

Supplementary Table S2: Identificaion of six methylation-driven genes by multivariable Cox regression analysis.

Supplementary Table S3: Compared the overall survival prediction and AUC values of 63 different combined models in the training set.

Supplementary Table S4: The C-index of TNM staging system and nomograms.

Supplementary Table S5: Compared the prognostic effect of four methylation-driven genes signature with other partially known biomarkers.

# I Supplementary Figures

## Supplementary Figure Legends

**Supplementary Figure S1. Flowchart of the research.** Identifying and validating methylation-driven genes, developing the risk score model and analyzing the efficiency of the signature to predict prognostic outcomes. TCGA, The Cancer Genome Atlas; ROC, receiver operating characteristic; AUC, area under the curve; GEO, The Gene Expression Omnibus

**Supplementary Figure S2. Correlation between DNA methylation and gene expression of *ANXA9, BATF, RBP1,* and *SERPINA1* in the training dataset and validation dataset.** *ANXA9*, Annexin A family member 9; *BATF*, Basic Leucine Zipper ATF-Like Transcription Factor; *RBP1*, Retinol Binding Protein 1; *SERPINA1*, Serpin family A member 1. The vertical axis and the horizontal axis denote the mRNA level and DNA methylation level, respectively

**Supplementary Figure S3. The difference of expression levels of four methylation-driven genes between tumor tissue and normal tissue.**

**Supplementary Figure S4. Validation of four-gene risk score model in the GEO dataset. (A)** Distribution of risk scores in the high-risk and low-risk subgroups. **(B)** Survival overview in two high-risk and low-risk groups. **(C)** Heatmap of the four-gene expression profiles corresponding risk scores in the high-risk and low-risk subgroups in the GEO database. **(D)** Comparison of OS between the high-risk score and low-risk score groups. OS, overall survival

**Supplementary Figure S5. Kaplan–Meier and ROC analyses of CRC patients based on different age, gender, and TNM staging subgroups in the training set.** Kaplan–Meier analysis was performed to estimate the differences in OS between the low-risk and high-risk patients. ROC curves of the methylation-driven gene signature were used to demonstrate the sensitivity and specificity in predicting the OS of CRC patients. OS, overall survival; ROC, receiver operating characteristic; CRC, colorectal cancer

**Supplementary Figure S6. Kaplan–Meier and ROC analyses of CRC patients based on different age, gender, and TNM staging subgroups in the testing set.** Kaplan–Meier analysis was performed to estimate the differences in OS between the low-risk and high-risk patients. ROC curves of the methylation-driven gene signature were used to demonstrate the sensitivity and specificity in predicting the OS of CRC patients. OS, overall survival; ROC, receiver operating characteristic; CRC, colorectal cancer

**Supplementary Figure S7. Comparison of ROC curves between the signature and other known biomarkers in predicting 8-year OS of CRC patients.** OS, overall survival; ROC, receiver operating characteristic; CRC, colorectal cancer

**Supplementary Figure S8. Gene set enrichment analysis of candidate four methylation-driven genes.** (A, B) GO (biological process) and KEGG pathway of *BATF*. (C, D) GO (biological process) and KEGG pathway of *PHYHIPL*. (E, F) GO (biological process) and KEGG pathway of *PNPLA4*. (G, H) GO (biological process) and KEGG pathway of *RBP1*. KEGG, Kyoto Encyclopedia of Genes and Genomes; GO, Gene Ontology; NES, normalized enrichment score; FDR, false discovery rate.

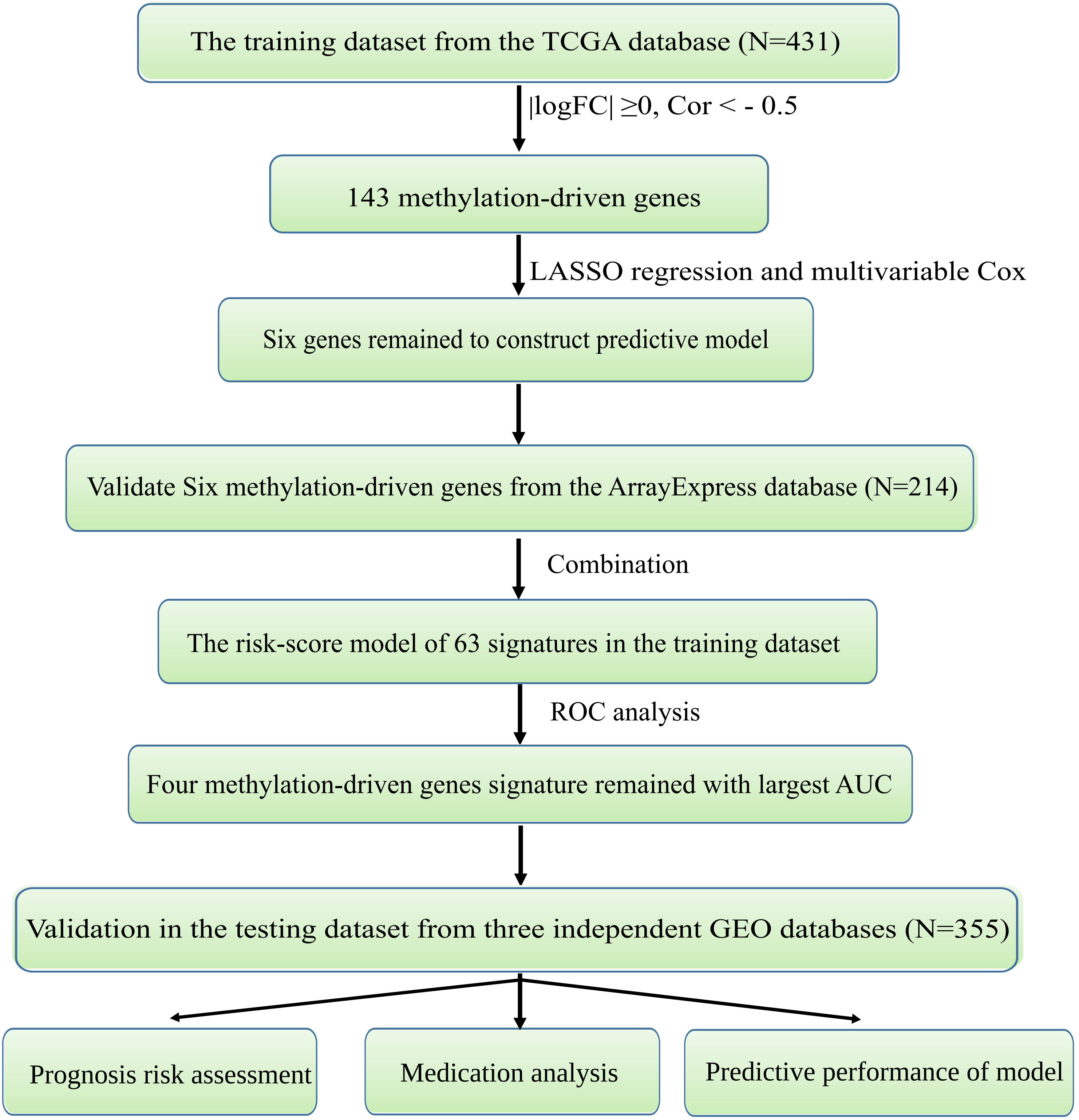

**Supplementary Figure S1**

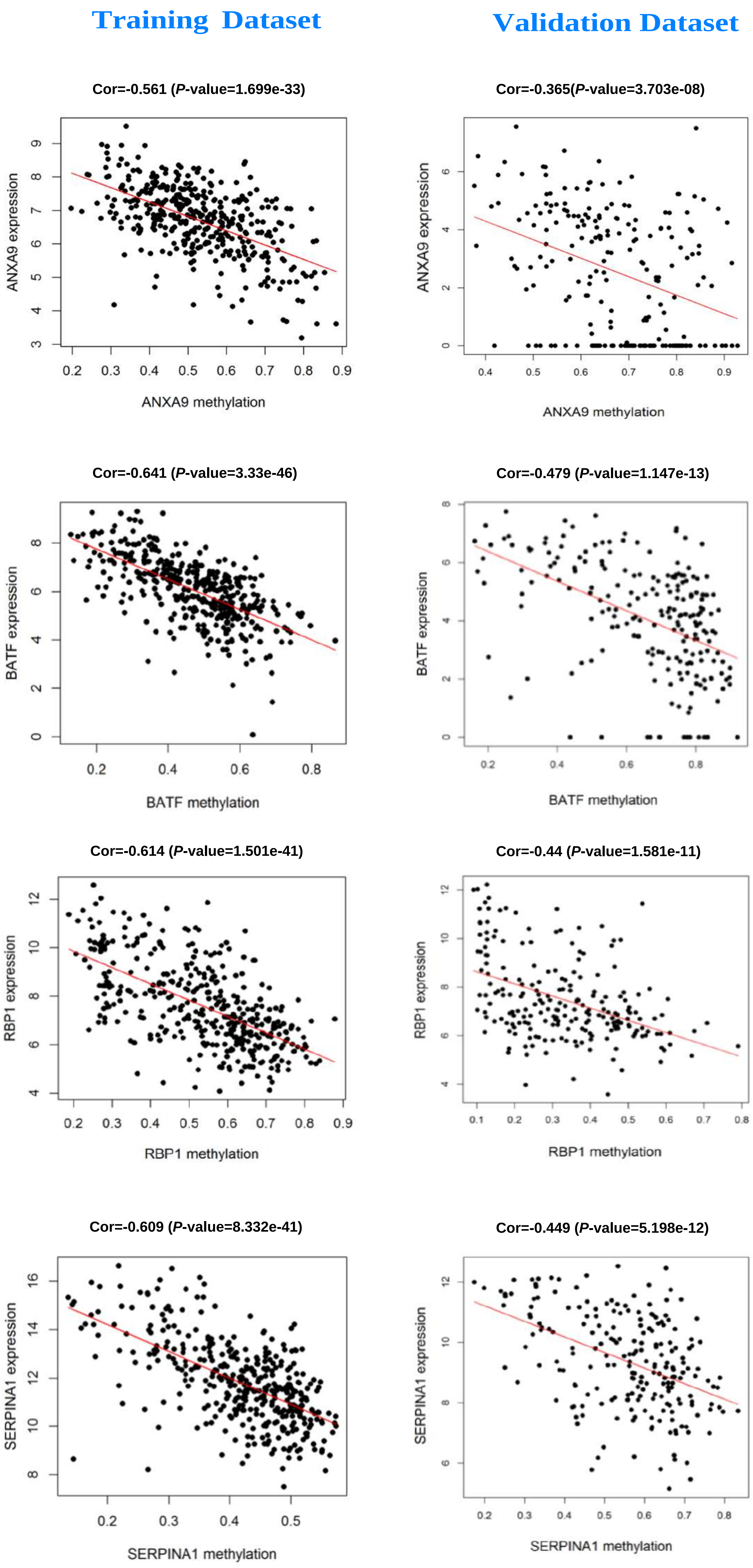

**Supplementary Figure S2**

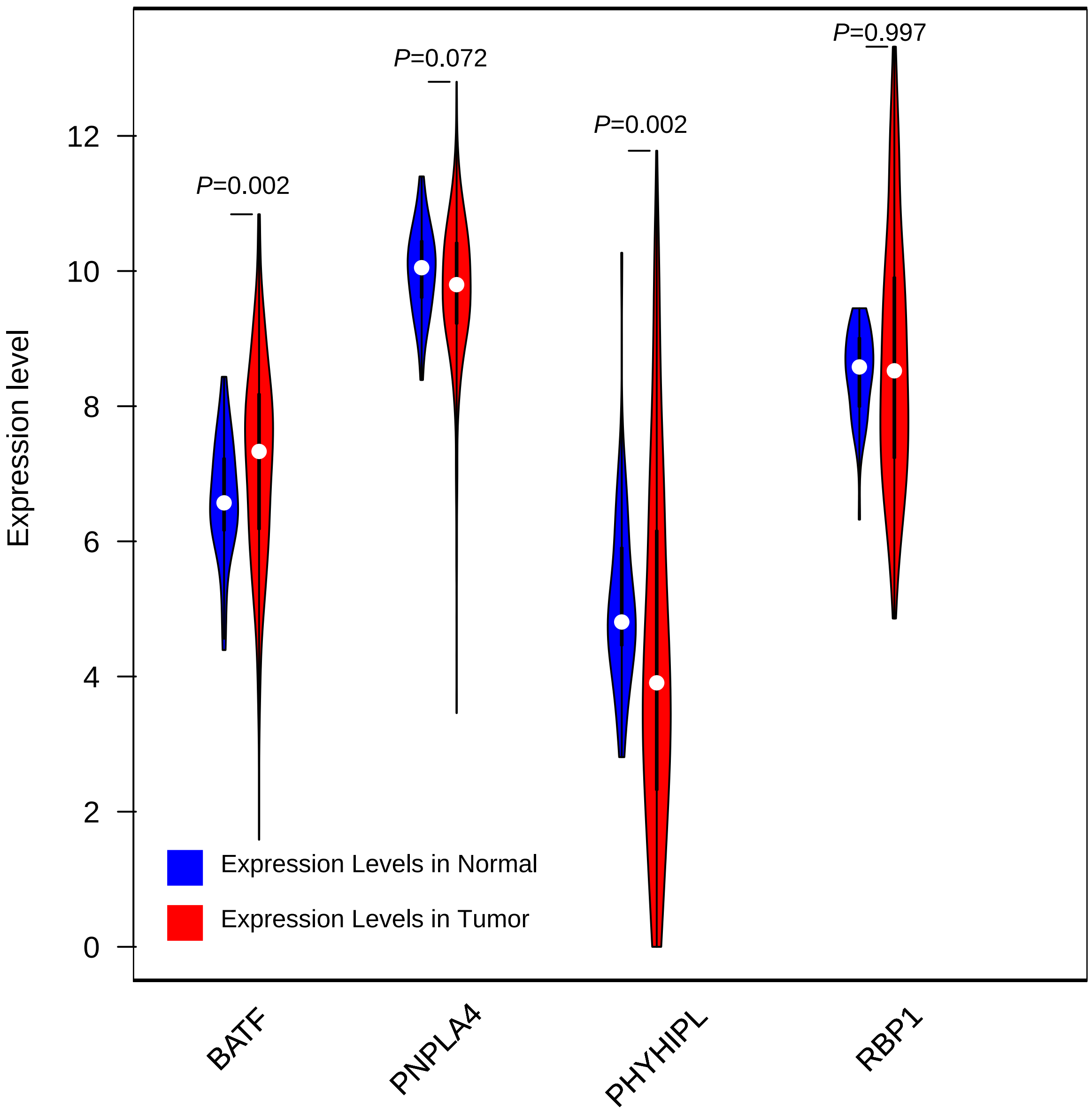

**Supplementary Figure S3**

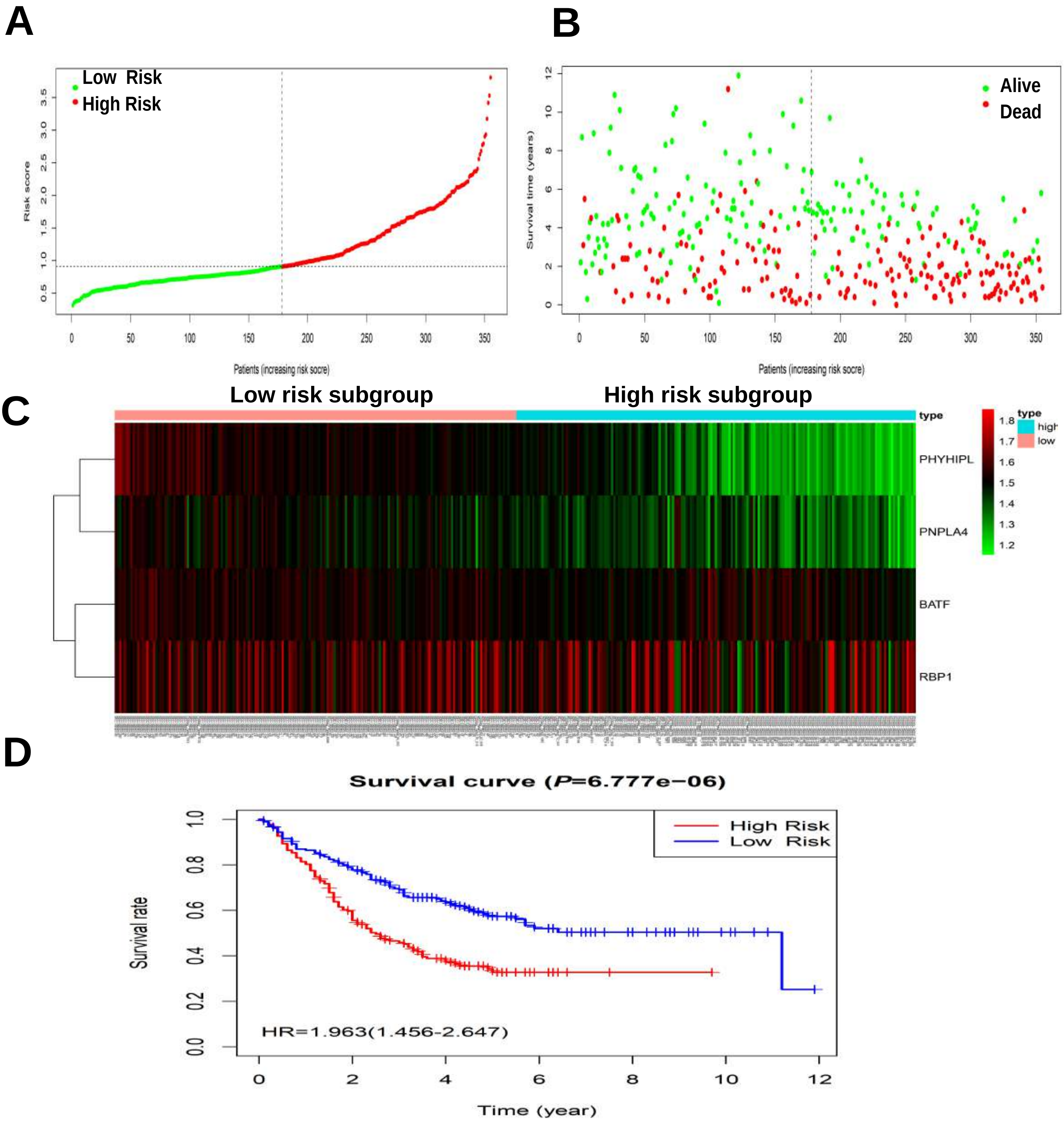

**Supplementary Figure S4**

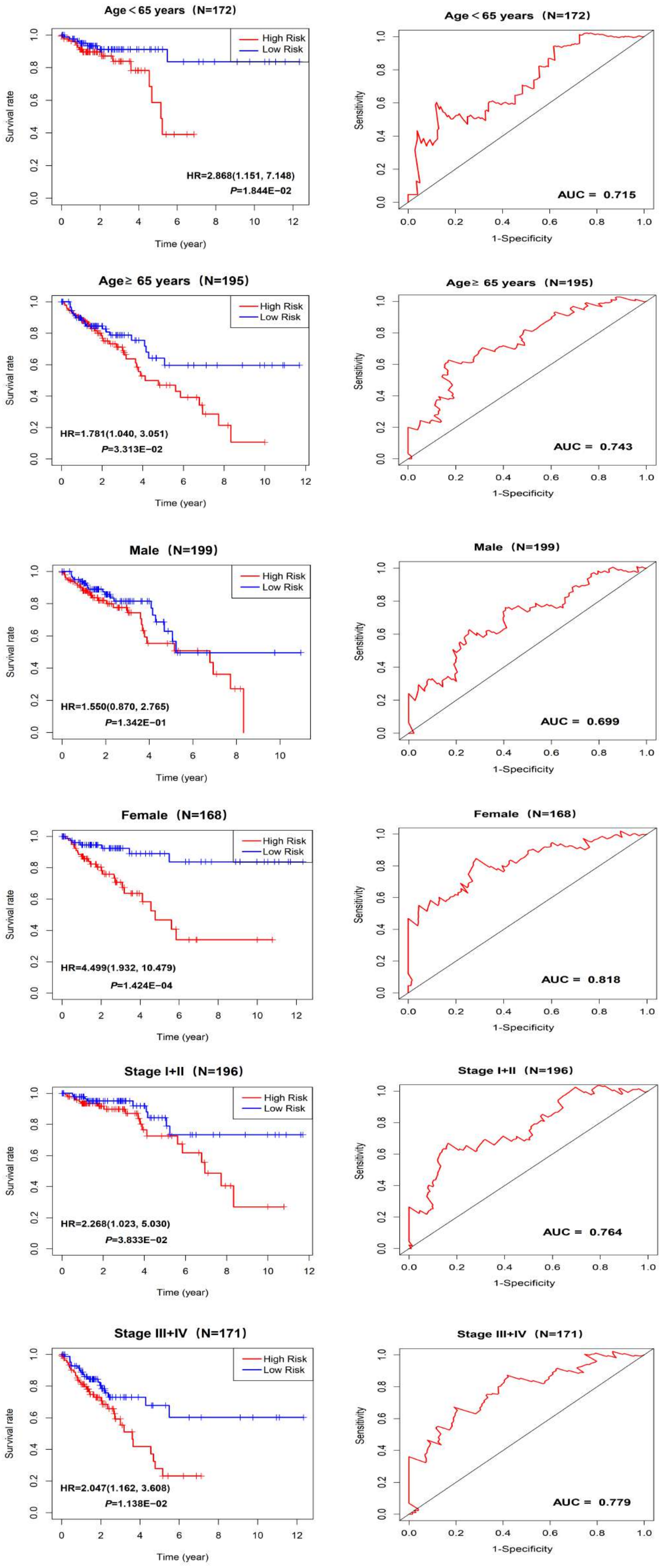

**Supplementary Figure S5**

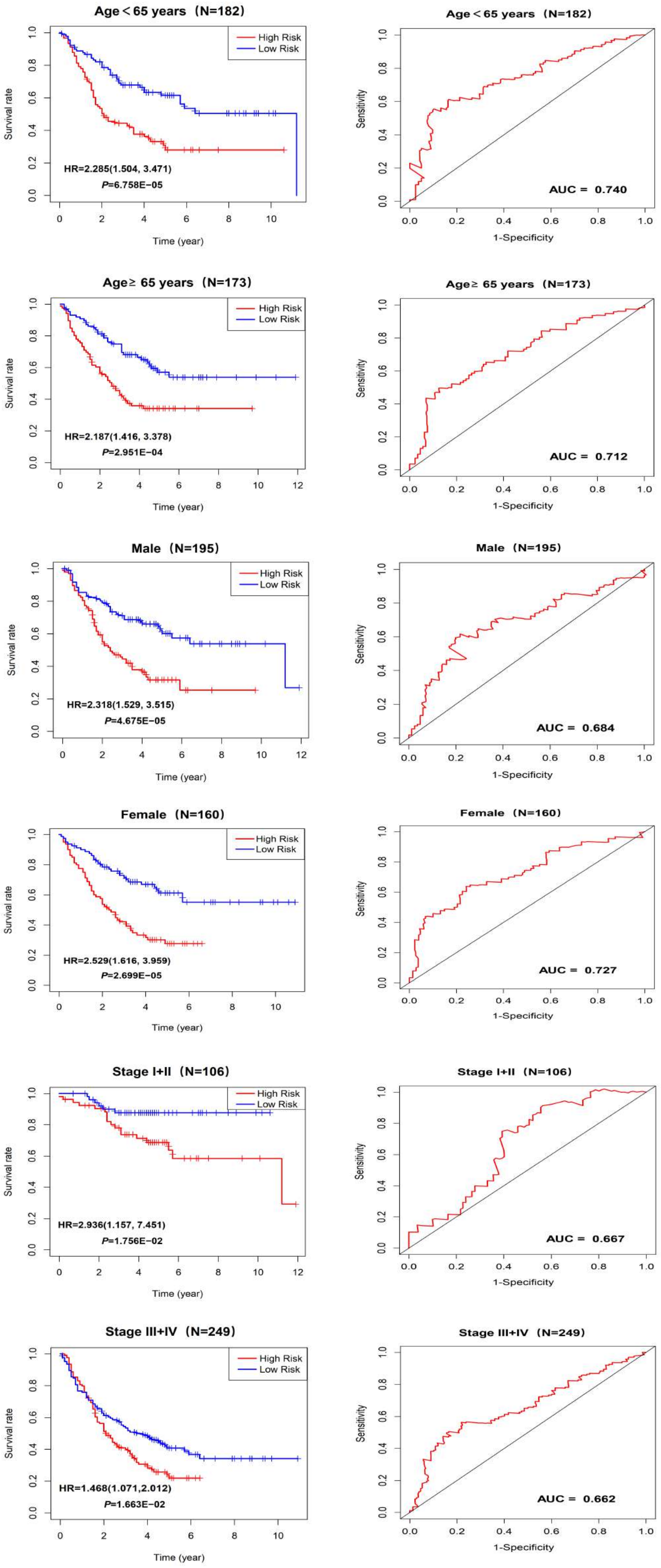

**Supplementary Figure S6**

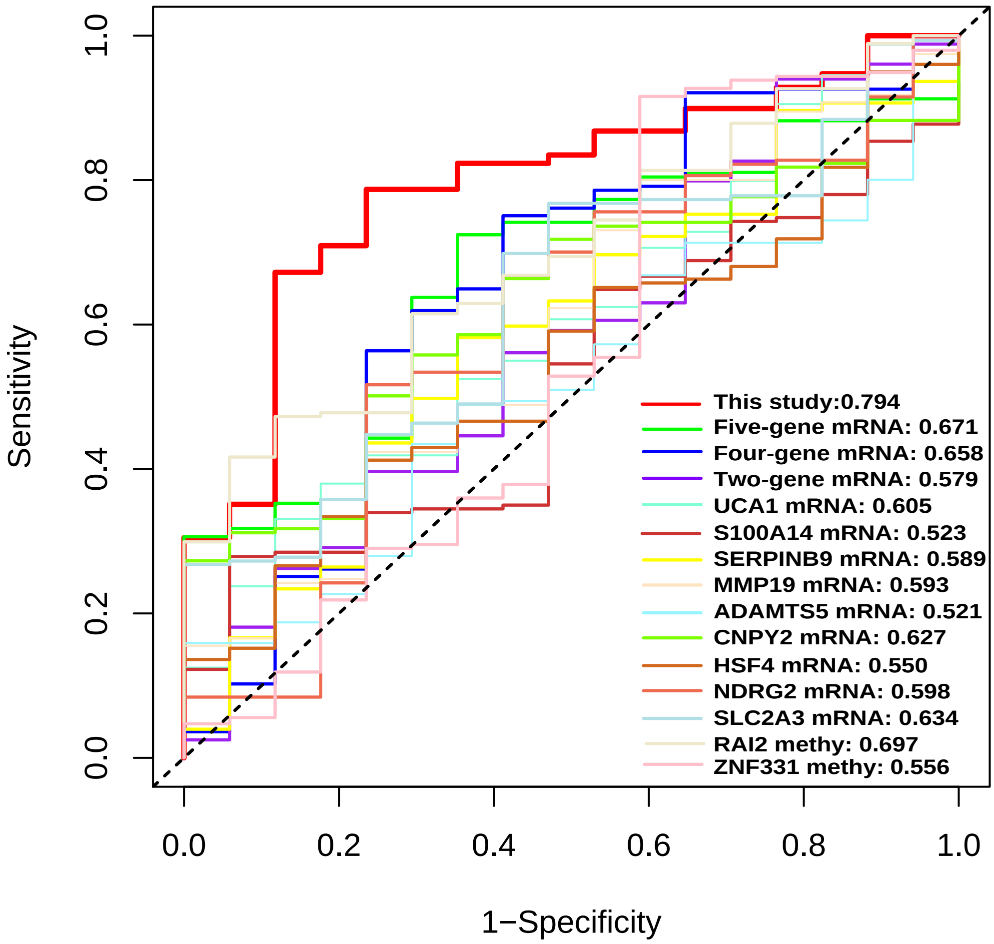

**Supplementary Figure S7**

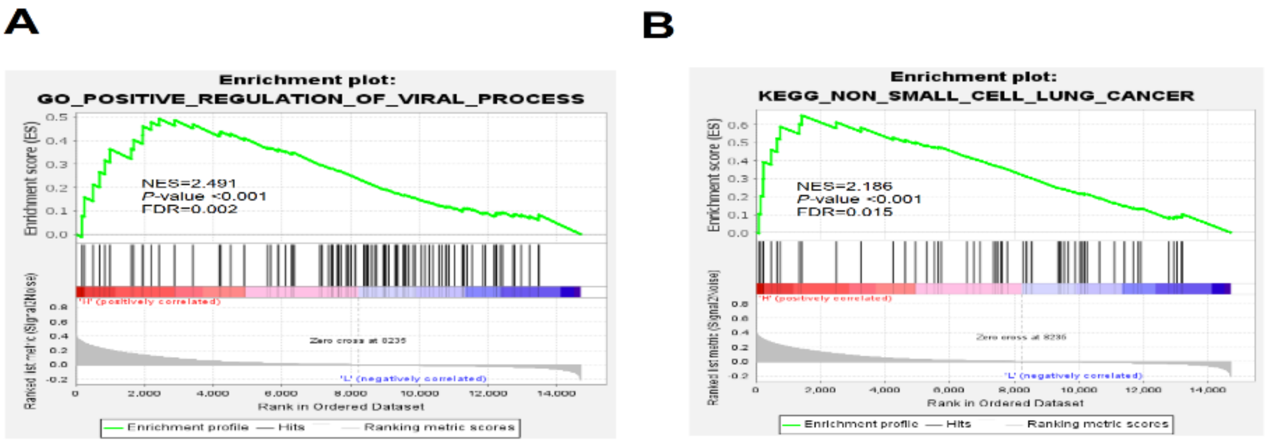

**BATF** **BATF**

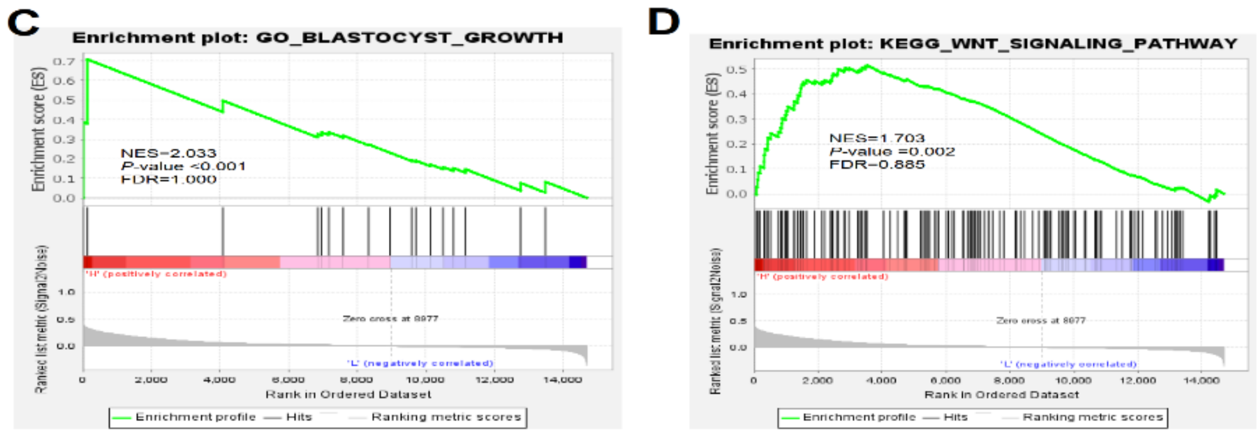

**PHYHIPL** **PHYHIPL**

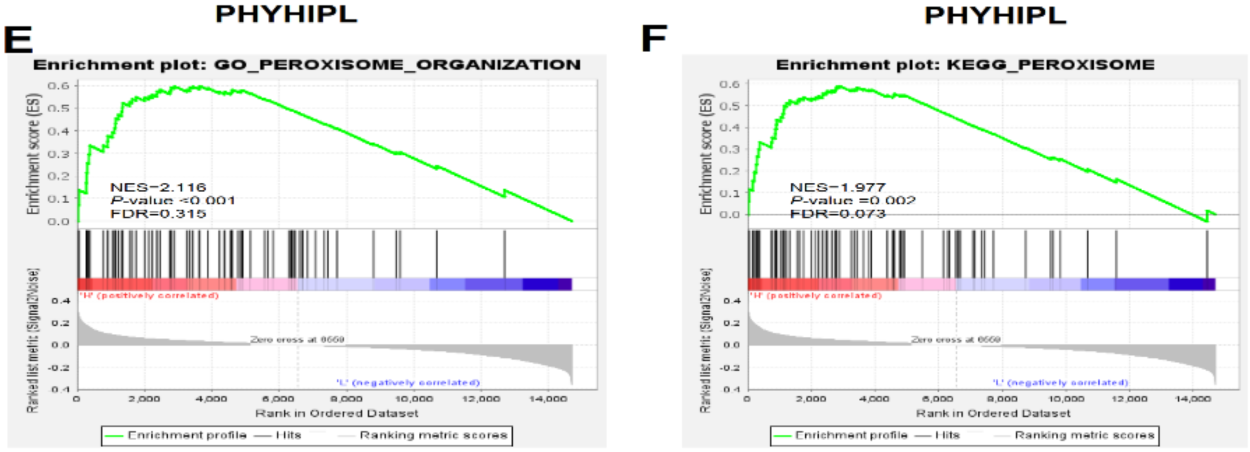

**PNPLA4** **PNPLA4**

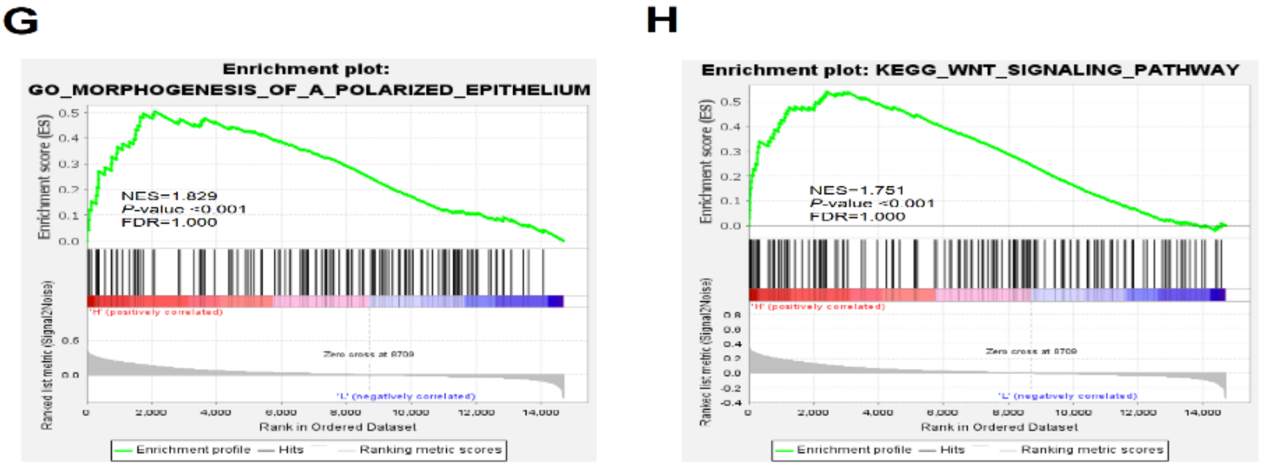

**RBP1** **RBP1**

**Supplementary Figure S8**

## II Supplementary Tables

**Table S1. 143 epigenetic drivers were identified by MethylMix.**

| Gene Symbol | NormalMean | TumorMean | logFC | *P*-Value | adjust *P*-Value | cor | cor *P*-value |
|---|---|---|---|---|---|---|---|
| ABCC2 | 0.736 | 0.618 | -0.253 | 0.000 | 0.000 | -0.583 | 0.000 |
| ADAL | 0.059 | 0.094 | 0.686 | 0.000 | 0.015 | -0.559 | 0.000 |
| AIM2 | 0.724 | 0.454 | -0.672 | 0.000 | 0.000 | -0.514 | 0.000 |
| AKR1B1 | 0.130 | 0.473 | 1.868 | 0.000 | 0.000 | -0.620 | 0.000 |
| ANO6 | 0.083 | 0.110 | 0.406 | 0.000 | 0.000 | -0.508 | 0.000 |
| ANXA9 | 0.702 | 0.530 | -0.405 | 0.000 | 0.000 | -0.561 | 0.000 |
| AQP5 | 0.197 | 0.481 | 1.292 | 0.000 | 0.000 | -0.628 | 0.000 |
| ARHGDIB | 0.781 | 0.550 | -0.506 | 0.000 | 0.000 | -0.519 | 0.000 |
| B3GALNT1 | 0.209 | 0.383 | 0.874 | 0.000 | 0.000 | -0.510 | 0.000 |
| BATF | 0.589 | 0.470 | -0.325 | 0.000 | 0.000 | -0.641 | 0.000 |
| BST2 | 0.468 | 0.298 | -0.654 | 0.000 | 0.000 | -0.670 | 0.000 |
| C10orf99 | 0.442 | 0.654 | 0.564 | 0.000 | 0.000 | -0.586 | 0.000 |
| C3orf14 | 0.414 | 0.524 | 0.340 | 0.000 | 0.000 | -0.809 | 0.000 |
| C6orf15 | 0.807 | 0.715 | -0.174 | 0.000 | 0.000 | -0.547 | 0.000 |
| CADPS | 0.203 | 0.178 | -0.188 | 0.000 | 0.040 | -0.576 | 0.000 |
| CAPN8 | 0.908 | 0.571 | -0.671 | 0.000 | 0.000 | -0.505 | 0.000 |
| CD40 | 0.226 | 0.480 | 1.091 | 0.000 | 0.000 | -0.502 | 0.000 |
| CDHR1 | 0.128 | 0.190 | 0.573 | 0.000 | 0.000 | -0.583 | 0.000 |
| CDK20 | 0.141 | 0.118 | -0.248 | 0.000 | 0.000 | -0.611 | 0.000 |
| CEACAM6 | 0.386 | 0.251 | -0.619 | 0.000 | 0.000 | -0.635 | 0.000 |
| CEL | 0.629 | 0.504 | -0.319 | 0.000 | 0.001 | -0.795 | 0.000 |
| CELP | 0.747 | 0.535 | -0.480 | 0.000 | 0.000 | -0.704 | 0.000 |
| CFTR | 0.136 | 0.099 | -0.454 | 0.000 | 0.000 | -0.519 | 0.000 |
| CHFR | 0.040 | 0.239 | 2.560 | 0.000 | 0.000 | -0.839 | 0.000 |
| CIDEB | 0.497 | 0.636 | 0.354 | 0.000 | 0.000 | -0.517 | 0.000 |
| DAPP1 | 0.584 | 0.416 | -0.490 | 0.000 | 0.000 | -0.704 | 0.000 |
| DNAJC15 | 0.787 | 0.693 | -0.183 | 0.000 | 0.000 | -0.561 | 0.000 |
| ECHDC3 | 0.379 | 0.500 | 0.398 | 0.000 | 0.002 | -0.689 | 0.000 |
| ELAVL2 | 0.065 | 0.264 | 2.013 | 0.000 | 0.000 | -0.514 | 0.000 |
| ELF5 | 0.729 | 0.602 | -0.277 | 0.000 | 0.000 | -0.789 | 0.000 |
| ENPP3 | 0.679 | 0.768 | 0.177 | 0.000 | 0.000 | -0.630 | 0.000 |
| EREG | 0.434 | 0.332 | -0.385 | 0.000 | 0.000 | -0.776 | 0.000 |
| FAM131A | 0.364 | 0.391 | 0.102 | 0.000 | 0.000 | -0.557 | 0.000 |
| FAM155B | 0.234 | 0.398 | 0.766 | 0.000 | 0.002 | -0.573 | 0.000 |
| FAM3D | 0.470 | 0.411 | -0.195 | 0.000 | 0.007 | -0.586 | 0.000 |
| FCGBP | 0.761 | 0.693 | -0.134 | 0.000 | 0.000 | -0.530 | 0.000 |
| FGF2 | 0.626 | 0.739 | 0.238 | 0.000 | 0.000 | -0.545 | 0.000 |
| FLJ32063 | 0.145 | 0.327 | 1.173 | 0.000 | 0.000 | -0.731 | 0.000 |
| FUZ | 0.046 | 0.173 | 1.926 | 0.000 | 0.000 | -0.651 | 0.000 |
| FZD10 | 0.161 | 0.341 | 1.080 | 0.000 | 0.000 | -0.578 | 0.000 |
| GBGT1 | 0.513 | 0.642 | 0.325 | 0.000 | 0.000 | -0.576 | 0.000 |
| GIPC2 | 0.234 | 0.184 | -0.346 | 0.000 | 0.000 | -0.532 | 0.000 |
| GPX2 | 0.603 | 0.450 | -0.422 | 0.000 | 0.000 | -0.543 | 0.000 |
| GPX7 | 0.272 | 0.419 | 0.626 | 0.000 | 0.000 | -0.607 | 0.000 |
| GYPC | 0.534 | 0.654 | 0.293 | 0.000 | 0.000 | -0.533 | 0.000 |
| HABP2 | 0.840 | 0.670 | -0.325 | 0.000 | 0.000 | -0.601 | 0.000 |
| HNF4A | 0.427 | 0.323 | -0.402 | 0.000 | 0.000 | -0.530 | 0.000 |
| HYDIN | 0.398 | 0.566 | 0.510 | 0.000 | 0.000 | -0.561 | 0.000 |
| IFITM1 | 0.593 | 0.398 | -0.577 | 0.000 | 0.000 | -0.684 | 0.000 |
| INPP1 | 0.562 | 0.446 | -0.334 | 0.000 | 0.000 | -0.522 | 0.000 |
| INPP5D | 0.587 | 0.377 | -0.639 | 0.000 | 0.000 | -0.769 | 0.000 |
| IRAK3 | 0.372 | 0.477 | 0.358 | 0.000 | 0.000 | -0.583 | 0.000 |

| | | | | | | | |
|---|---|---|---|---|---|---|---|
| IRX2 | 0.184 | 0.403 | 1.130 | 0.000 | 0.000 | -0.635 | 0.000 |
| KIF25 | 0.796 | 0.634 | -0.330 | 0.000 | 0.023 | -0.613 | 0.000 |
| KRBA1 | 0.456 | 0.702 | 0.621 | 0.000 | 0.000 | -0.693 | 0.000 |
| KRT20 | 0.517 | 0.369 | -0.485 | 0.000 | 0.000 | -0.560 | 0.000 |
| KRT23 | 0.763 | 0.546 | -0.484 | 0.000 | 0.000 | -0.559 | 0.000 |
| KRT7 | 0.448 | 0.604 | 0.430 | 0.000 | 0.000 | -0.531 | 0.000 |
| LCMT2 | 0.059 | 0.094 | 0.686 | 0.000 | 0.015 | -0.522 | 0.000 |
| LOC286467 | 0.561 | 0.326 | -0.784 | 0.000 | 0.000 | -0.549 | 0.000 |
| LRRC4 | 0.078 | 0.444 | 2.508 | 0.000 | 0.000 | -0.552 | 0.000 |
| LY6G6D | 0.458 | 0.345 | -0.407 | 0.000 | 0.000 | -0.728 | 0.000 |
| MEIS3P1 | 0.617 | 0.703 | 0.188 | 0.000 | 0.000 | -0.629 | 0.000 |
| MIA | 0.874 | 0.628 | -0.477 | 0.000 | 0.000 | -0.583 | 0.000 |
| NINL | 0.107 | 0.302 | 1.501 | 0.000 | 0.005 | -0.623 | 0.000 |
| NMRAL1 | 0.146 | 0.121 | -0.270 | 0.000 | 0.000 | -0.549 | 0.000 |
| NPC1L1 | 0.758 | 0.681 | -0.154 | 0.000 | 0.000 | -0.634 | 0.000 |
| NUDT12 | 0.297 | 0.247 | -0.266 | 0.000 | 0.006 | -0.670 | 0.000 |
| PGC | 0.833 | 0.729 | -0.193 | 0.000 | 0.000 | -0.509 | 0.000 |
| PHYHIPL | 0.095 | 0.290 | 1.611 | 0.000 | 0.000 | -0.531 | 0.000 |
| PIGR | 0.389 | 0.572 | 0.555 | 0.000 | 0.000 | -0.742 | 0.000 |
| PIPOX | 0.447 | 0.216 | -1.047 | 0.000 | 0.000 | -0.629 | 0.000 |
| PKIA | 0.086 | 0.380 | 2.146 | 0.000 | 0.000 | -0.657 | 0.000 |
| PNPLA4 | 0.173 | 0.167 | -0.050 | 0.000 | 0.000 | -0.508 | 0.000 |
| PRKY | 0.349 | 0.254 | -0.455 | 0.000 | 0.015 | -0.772 | 0.000 |
| PTK7 | 0.249 | 0.337 | 0.435 | 0.000 | 0.000 | -0.590 | 0.000 |
| QPCT | 0.417 | 0.367 | -0.186 | 0.000 | 0.000 | -0.525 | 0.000 |
| RAB32 | 0.212 | 0.181 | -0.228 | 0.000 | 0.000 | -0.567 | 0.000 |
| RARRES3 | 0.681 | 0.524 | -0.379 | 0.000 | 0.000 | -0.562 | 0.000 |
| RBP1 | 0.415 | 0.536 | 0.368 | 0.000 | 0.000 | -0.614 | 0.000 |
| RNF212 | 0.590 | 0.706 | 0.257 | 0.000 | 0.000 | -0.570 | 0.000 |
| RPL39L | 0.099 | 0.383 | 1.957 | 0.000 | 0.000 | -0.674 | 0.000 |
| SERP2 | 0.321 | 0.447 | 0.479 | 0.000 | 0.006 | -0.818 | 0.000 |
| SERPINA1 | 0.528 | 0.417 | -0.340 | 0.000 | 0.000 | -0.609 | 0.000 |
| SLC43A3 | 0.408 | 0.554 | 0.440 | 0.000 | 0.000 | -0.615 | 0.000 |
| SPAG16 | 0.144 | 0.238 | 0.728 | 0.000 | 0.000 | -0.768 | 0.000 |
| SRPX2 | 0.682 | 0.505 | -0.434 | 0.000 | 0.000 | -0.698 | 0.000 |
| SULT4A1 | 0.291 | 0.506 | 0.799 | 0.000 | 0.000 | -0.531 | 0.000 |
| TBX18 | 0.172 | 0.475 | 1.466 | 0.000 | 0.000 | -0.738 | 0.000 |
| TMEM106A | 0.078 | 0.302 | 1.959 | 0.000 | 0.028 | -0.700 | 0.000 |
| TMEM173 | 0.235 | 0.205 | -0.201 | 0.000 | 0.036 | -0.644 | 0.000 |
| TMEM220 | 0.442 | 0.636 | 0.524 | 0.000 | 0.000 | -0.589 | 0.000 |
| TMEM71 | 0.728 | 0.617 | -0.239 | 0.000 | 0.019 | -0.603 | 0.000 |
| VSIG2 | 0.550 | 0.684 | 0.315 | 0.000 | 0.000 | -0.602 | 0.000 |
| WDR35 | 0.147 | 0.131 | -0.167 | 0.000 | 0.000 | -0.608 | 0.000 |
| ZFP28 | 0.070 | 0.403 | 2.524 | 0.000 | 0.000 | -0.746 | 0.000 |
| ZFP82 | 0.140 | 0.448 | 1.681 | 0.000 | 0.000 | -0.714 | 0.000 |
| ZIK1 | 0.400 | 0.621 | 0.635 | 0.000 | 0.000 | -0.536 | 0.000 |
| ZNF134 | 0.044 | 0.281 | 2.681 | 0.000 | 0.000 | -0.752 | 0.000 |
| ZNF141 | 0.086 | 0.175 | 1.020 | 0.000 | 0.002 | -0.733 | 0.000 |
| ZNF256 | 0.049 | 0.274 | 2.471 | 0.000 | 0.000 | -0.789 | 0.000 |
| ZNF264 | 0.393 | 0.477 | 0.279 | 0.000 | 0.000 | -0.622 | 0.000 |
| ZNF285 | 0.119 | 0.354 | 1.574 | 0.000 | 0.000 | -0.790 | 0.000 |
| ZNF287 | 0.083 | 0.214 | 1.361 | 0.000 | 0.000 | -0.616 | 0.000 |
| ZNF300 | 0.343 | 0.506 | 0.559 | 0.000 | 0.000 | -0.795 | 0.000 |
| ZNF304 | 0.108 | 0.405 | 1.902 | 0.000 | 0.000 | -0.743 | 0.000 |
| ZNF331 | 0.378 | 0.556 | 0.556 | 0.000 | 0.000 | -0.616 | 0.000 |
| ZNF334 | 0.304 | 0.606 | 0.995 | 0.000 | 0.000 | -0.541 | 0.000 |

| | | | | | | | |
|---|---|---|---|---|---|---|---|
| ZNF347 | 0.164 | 0.381 | 1.215 | 0.000 | 0.000 | -0.701 | 0.000 |
| ZNF354C | 0.079 | 0.323 | 2.024 | 0.000 | 0.000 | -0.611 | 0.000 |
| ZNF415 | 0.274 | 0.500 | 0.868 | 0.000 | 0.000 | -0.680 | 0.000 |
| ZNF43 | 0.147 | 0.431 | 1.549 | 0.000 | 0.000 | -0.778 | 0.000 |
| ZNF461 | 0.136 | 0.294 | 1.108 | 0.000 | 0.000 | -0.623 | 0.000 |
| ZNF471 | 0.155 | 0.457 | 1.560 | 0.000 | 0.000 | -0.630 | 0.000 |
| ZNF480 | 0.057 | 0.113 | 0.982 | 0.000 | 0.009 | -0.734 | 0.000 |
| ZNF506 | 0.263 | 0.305 | 0.215 | 0.000 | 0.002 | -0.547 | 0.000 |
| ZNF525 | 0.157 | 0.265 | 0.752 | 0.000 | 0.000 | -0.666 | 0.000 |
| ZNF528 | 0.116 | 0.412 | 1.829 | 0.000 | 0.000 | -0.713 | 0.000 |
| ZNF529 | 0.217 | 0.390 | 0.847 | 0.000 | 0.000 | -0.641 | 0.000 |
| ZNF543 | 0.047 | 0.320 | 2.776 | 0.000 | 0.000 | -0.770 | 0.000 |
| ZNF547 | 0.040 | 0.128 | 1.675 | 0.000 | 0.000 | -0.657 | 0.000 |
| ZNF549 | 0.264 | 0.513 | 0.957 | 0.000 | 0.000 | -0.807 | 0.000 |
| ZNF568 | 0.127 | 0.458 | 1.856 | 0.000 | 0.000 | -0.551 | 0.000 |
| ZNF569 | 0.201 | 0.387 | 0.942 | 0.000 | 0.000 | -0.664 | 0.000 |
| ZNF570 | 0.172 | 0.364 | 1.083 | 0.000 | 0.000 | -0.747 | 0.000 |
| ZNF582 | 0.188 | 0.517 | 1.458 | 0.000 | 0.000 | -0.600 | 0.000 |
| ZNF583 | 0.063 | 0.150 | 1.244 | 0.000 | 0.005 | -0.627 | 0.000 |
| ZNF625 | 0.044 | 0.443 | 3.329 | 0.000 | 0.000 | -0.563 | 0.000 |
| ZNF655 | 0.042 | 0.229 | 2.435 | 0.000 | 0.000 | -0.815 | 0.000 |
| ZNF662 | 0.423 | 0.636 | 0.588 | 0.000 | 0.000 | -0.621 | 0.000 |
| ZNF677 | 0.381 | 0.615 | 0.691 | 0.000 | 0.000 | -0.501 | 0.000 |
| ZNF682 | 0.056 | 0.236 | 2.066 | 0.000 | 0.000 | -0.768 | 0.000 |
| ZNF75A | 0.245 | 0.513 | 1.067 | 0.000 | 0.000 | -0.550 | 0.000 |
| ZNF772 | 0.266 | 0.451 | 0.763 | 0.000 | 0.000 | -0.618 | 0.000 |
| ZNF793 | 0.043 | 0.424 | 3.290 | 0.000 | 0.000 | -0.737 | 0.000 |
| ZNF813 | 0.093 | 0.274 | 1.551 | 0.000 | 0.000 | -0.711 | 0.000 |
| ZNF829 | 0.127 | 0.458 | 1.856 | 0.000 | 0.000 | -0.555 | 0.000 |
| ZNF83 | 0.137 | 0.258 | 0.916 | 0.000 | 0.001 | -0.565 | 0.000 |
| ZNF844 | 0.071 | 0.141 | 0.986 | 0.000 | 0.002 | -0.604 | 0.000 |
| ZNF85 | 0.285 | 0.537 | 0.917 | 0.000 | 0.000 | -0.599 | 0.000 |
| ZNF880 | 0.125 | 0.419 | 1.741 | 0.000 | 0.000 | -0.576 | 0.000 |
| ZSCAN18 | 0.373 | 0.502 | 0.429 | 0.000 | 0.000 | -0.660 | 0.000 |
| ZSCAN23 | 0.144 | 0.477 | 1.729 | 0.000 | 0.000 | -0.579 | 0.000 |

## Table S2. Identificaion of six methylation-driven genes by multivariable Cox regression analysis.

| Gene symbol | Coefficient[a] | HR | HR(95%Low) | HR(95%High) | *P* -value[a] |
|---|---|---|---|---|---|
| ANXA9 | 0.261 | 1.298 | 1.038 | 1.623 | 0.022 |
| BATF | 0.247 | 1.281 | 1.084 | 1.513 | 0.004 |
| PHYHIPL | 0.136 | 1.146 | 1.035 | 1.268 | 0.009 |
| PNPLA4 | -0.224 | 0.799 | 0.658 | 0.970 | 0.023 |
| RBP1 | -0.232 | 0.793 | 0.688 | 0.914 | 0.001 |
| SERPINA1 | -0.195 | 0.823 | 0.713 | 0.950 | 0.008 |

[a] Derived from the multivariable Cox regression analysis in the training set.

**Table S3. Compared the overall survival prediction and AUC values of 63 different combined models in the training set.**

| Combined Model | | Overall Survival | | | | |
|---|---|---|---|---|---|---|
| | | **HR** | **HR(95%Low)** | **HR(95%High)** | ***P* -value** | **AUC$^{a}$** |
| One Gene Model | ANXA9 | 1.420 | 0.929 | 2.173 | 0.104 | 0.569 (5) |
| | BATF | 1.763 | 1.144 | 2.717 | 0.009 | 0.701 |
| | PHYHIPL | 1.358 | 0.890 | 2.070 | 0.154 | 0.677 (6) |
| | PNPLA4 | 1.466 | 0.960 | 2.239 | 0.075 | 0.731 |
| | RBP1 | 1.103 | 0.726 | 1.676 | 0.647 | 0.652 |
| | SERPINA1 | 1.730 | 1.128 | 2.653 | 0.011 | 0.608 |
| Two Genes Model | A-B | 2.184 | 1.404 | 3.398 | 0.000 | 0.645 |
| | A-P1 | 1.583 | 1.032 | 2.428 | 0.034 | 0.636 (6) |
| | A-P2 | 1.845 | 1.197 | 2.843 | 0.005 | 0.660 |
| | A-R | 1.628 | 1.065 | 2.487 | 0.023 | 0.608 (5) |
| | A-S | 1.860 | 1.207 | 2.865 | 0.004 | 0.567 |
| | B-P1 | 2.116 | 1.367 | 3.277 | 0.001 | 0.699 |
| | B-P2 | 1.883 | 1.222 | 2.901 | 0.004 | 0.772 |
| | B-R | 1.728 | 1.126 | 2.653 | 0.011 | 0.811 |
| | B-S | 2.305 | 1.475 | 3.600 | 0.000 | 0.724 |
| | P1-R | 1.563 | 1.025 | 2.384 | 0.004 | 0.671 (6) |
| | P1-S | 1.637 | 1.069 | 2.506 | 0.022 | 0.649 (6) |
| | P2-S | 1.966 | 1.276 | 3.028 | 0.002 | 0.705 |
| | P2-R | 1.592 | 1.043 | 2.430 | 0.030 | 0.752 |
| | P1-P2 | 1.587 | 1.036 | 2.430 | 0.032 | 0.710 |
| | R-S | 1.716 | 1.121 | 2.627 | 0.012 | 0.689 |
| Three Genes Model | A-B-P1 | 1.991 | 1.288 | 3.076 | 0.002 | 0.673 (6) |
| | A-B-P2 | 2.527 | 1.598 | 3.997 | 0.000 | 0.742 |
| | A-B-R | 2.227 | 1.437 | 3.451 | 0.000 | 0.704 |
| | A-B-S | 2.414 | 1.539 | 3.785 | 0.000 | 0.691 |
| | A-P1-P2 | 1.827 | 1.181 | 2.826 | 0.006 | 0.664 |
| | A-P1-R | 1.973 | 1.285 | 3.031 | 0.002 | 0.683 (5) |
| | A-P1-S | 1.687 | 1.100 | 2.589 | 0.015 | 0.645 |
| | A-P2-R | 1.940 | 1.261 | 2.982 | 0.002 | 0.670 |
| | A-P2-S | 2.120 | 1.364 | 3.295 | 0.001 | 0.666 |
| | A-R-S | 2.015 | 1.309 | 3.101 | 0.001 | 0.625 |
| | B-P1-P2 | 1.872 | 1.212 | 2.891 | 0.004 | 0.803 |
| | B-P1-R | 1.692 | 1.101 | 2.601 | 0.015 | 0.832 |
| | B-P1-S | 2.445 | 1.562 | 3.826 | 0.000 | 0.728 |
| | B-P2-R | 1.723 | 1.122 | 2.648 | 0.012 | 0.823 |
| | B-P2-S | 2.559 | 1.625 | 4.031 | 0.000 | 0.776 |
| | B-R-S | 2.445 | 1.564 | 3.823 | 0.000 | 0.793 |
| | P1-P2-R | 2.037 | 1.323 | 3.139 | 0.001 | 0.749 (7) |
| | P1-P2-S | 1.977 | 1.279 | 3.056 | 0.002 | 0.698 |
| | P1-R-S | 1.928 | 1.255 | 2.962 | 0.002 | 0.705 |
| | P2-R-S | 1.629 | 1.065 | 2.493 | 0.023 | 0.746 |
| Four Genes Model | P1-P2-R-S | 1.902 | 1.240 | 2.918 | 0.003 | 0.759 |
| | B-P2-R-S | 2.739 | 1.736 | 4.320 | 0.000 | 0.822 |
| | B-P1-R-S | 2.301 | 1.477 | 3.583 | 0.000 | 0.808 |
| | B-P1-P2-S | 2.459 | 1.567 | 3.860 | 0.000 | 0.780 |
| | B-P1-P2-R | 2.184 | 1.404 | 3.396 | 0.000 | 0.876 |
| | A-P2-R-S | 2.299 | 1.483 | 3.565 | 0.000 | 0.693 |
| | A-P1-R-S | 2.285 | 1.477 | 3.534 | 0.000 | 0.660 |
| | A-P1-P2-S | 1.926 | 1.247 | 2.977 | 0.003 | 0.669 |
| | A-P1-P2-R | 2.125 | 1.378 | 3.275 | 0.000 | 0.707 |
| | A-B-P2-S | 2.443 | 1.552 | 3.845 | 0.000 | 0.749 |
| | A-B-P2-R | 2.278 | 1.468 | 3.537 | 0.000 | 0.763 |

| | | | | | | |
|---|---|---|---|---|---|---|
| | A-B-P1-S | 2.296 | 1.477 | 3.569 | 0.000 | 0.703 |
| | A-B-P1-R | 2.365 | 1.514 | 3.693 | 0.000 | 0.745 |
| | A-B-R-S | 2.617 | 1.673 | 4.093 | 0.000 | 0.735 |
| | A-B-P1-P2 | 2.703 | 1.707 | 4.279 | 0.000 | 0.754 |
| Five Genes Model | B-P1-P2-R-S | 2.227 | 1.435 | 3.454 | 0.000 | 0.840 |
| | A-P1-P2-R-S | 1.819 | 1.186 | 2.790 | 0.005 | 0.724 |
| | A-B-P2-R-S | 3.240 | 2.035 | 5.160 | 0.000 | 0.778 |
| | A-B-P1-R-S | 2.809 | 1.779 | 4.435 | 0.000 | 0.761 |
| | A-B-P1-P2-S | 2.533 | 1.608 | 3.989 | 0.000 | 0.762 |
| | A-B-P1-P2-R | 2.573 | 1.645 | 4.023 | 0.000 | 0.804 |
| Six Genes Model | A-B-P1-P2-R-S | 2.648 | 1.688 | 4.155 | 0.000 | 0.796 |

Note:"A" means ANXA9, "B" means BATF, "P1" means PHYHIPL, "P2" means PNPLA4, "R" means RBP1, "S" me
SEPRINA1. "(5)" means predicting 5-year overall survival of patients

[a]=AUC based on the ROC curves for the sensitivity and specificity of different signatures in predicting 9-year overall survival of patients.

## Table S4. The C-index of TNM staging system and nomograms.

| **Models** | **Training set (N=367)** | | **Testing set (N=355)** | |
|---|---|---|---|---|
| | C-index (95%CI) | *P* -value | C-index (95%CI) | *P* -value |
| TNM staging | 0.719 (0.654-0.783) | <0.001 | 0.706 (0.669-0.743) | <0.001 |
| Nomogram | 0.747 (0.687-0.807) | <0.001 | 0.707 (0.670-0.743) | <0.001 |

# Table S5. Compared the prognostic effect of four methylation-driven genes signature with other partially known biomarkers.

| Signature | AUC | 95% CI of AUC | Type | *P* value[a] | Ref[b] |
|---|---|---|---|---|---|
| This study | 0.794 | 0.681-0.907 | Protein coding | | This study |
| Five-gene mRNA | 0.671 | 0.529-0.813 | Protein coding | 0.182 | [1] |
| Four-gene mRNA | 0.658 | 0.501-0.816 | Protein coding | 0.211 | [2] |
| Two-gene mRNA | 0.579 | 0.423-0.735 | Protein coding | 0.040 | [3] |
| UCA1 | 0.605 | 0.456-0.754 | Protein coding | 0.030 | [4] |
| S100A14 | 0.523 | 0.382-0.660 | Protein coding | 0.004 | [5] |
| SERPINB9 | 0.589 | 0.437-0.742 | Protein coding | 0.009 | [6] |
| MMP19 | 0.593 | 0.440-0.746 | Protein coding | 0.025 | [7] |
| ADAMTS5 | 0.521 | 0.375-0.668 | Protein coding | 0.001 | [8] |
| CNPY2 | 0.627 | 0.495-0.760 | Protein coding | 0.064 | [9] |
| HSF4 | 0.550 | 0.403-0.697 | Protein coding | 0.008 | [10] |
| NDRG2 | 0.598 | 0.437-0.758 | Protein coding | 0.028 | [11] |
| SLC2A3 | 0.634 | 0.495-0.773 | Protein coding | 0.087 | [12] |
| RAI2 | 0.697 | 0.571-0.823 | Methylation | 0.223 | [13] |
| ZNF331 | 0.556 | 0.377-0.734 | Methylation | 0.018 | [14] |

[a]:in the statistical comparison (Z test) between AUC value of corresponding signature and " this study" signature.

[b]:Additional References:

[1]. Sun G, Li Y, Peng Y, et al. Identification of a five-gene signature with prognostic value in colorectal cancer. Journal of cellular physiology. 2019;234(4):3829-36.

[2]. Li X, Zhang Q, Zhao L, et al. A Combined four-mRNA Signature Associated with Lymphatic Metastasis for Prognosis of Colorectal Cancer. Journal of Cancer. 2020;11(8):2139-49.

[3]. Abdel Raouf SM, Ibrahim TR, Abdelaziz LA, et al. Prognostic Value of TWIST1 and EZH2 Expression in Colon Cancer. Journal of gastrointestinal cancer. 2019.

[4]. Liu X, Liu X, Qiao T, et al. Prognostic and clinicopathological significance of long non-coding RNA UCA1 in colorectal cancer: Results from a meta-analysis. Medicine. 2019;98(48):e18031.

[5]. Diamantopoulou A, Mantas D, Kostakis ID, et al. A Clinicopathological Analysis of S100A14 Expression in Colorectal Cancer. In vivo (Athens, Greece). 2020;34(1):321-30.

[6]. Vycital O, Pitule P, Hosek P, et al. Expression of Serpin B9 as a Prognostic Factor of Colorectal Cancer. Anticancer research. 2019;39(11):6063-6.

[7]. Chen Z, Wu G, Ye F, et al. High expression of MMP19 is associated with poor prognosis in patients with colorectal cancer. BMC cancer. 2019;19(1):448.

[8]. Li J, Liao Y, Huang J, et al. Epigenetic silencing of ADAMTS5 is associated with increased invasiveness and poor survival in patients with colorectal cancer. Journal of cancer research and clinical oncology. 2018;144(2):215-27.

[9]. Peng J, Ou Q, Pan Z, Zhang R, Zhao Y, Deng Y, et al. Serum CNPY2 isoform 2 represents a novel biomarker for early detection of colorectal cancer. Aging. 2018;10(8):1921-31.

[10].Yang Y, Jin L, Zhang J, et al. High HSF4 expression is an independent indicator of poor overall survival and recurrence free survival in patients with primary colorectal cancer. IUBMB life. 2017;69(12):956-61.

[11].Chen W, Peng J, Ou Q, et al. Expression of NDRG2 in Human Colorectal Cancer and its Association with Prognosis. Journal of Cancer. 2019;10(15):3373-80.

[12].Kim E, Jung S, Park WS, et al. Upregulation of SLC2A3 gene and prognosis in colorectal carcinoma: analysis of TCGA data. BMC cancer. 2019;19(1):302.

[13].Yan W, Wu K, Herman JG, et al. Retinoic acid-induced 2 (RAI2) is a novel tumor suppressor, and promoter region methylation of RAI2 is a poor prognostic marker in colorectal cancer. Clinical epigenetics. 2018;10:69.

[14].Wang Y, He T, Herman JG, et al. Methylation of ZNF331 is an independent prognostic marker of colorectal cancer and promotes colorectal cancer growth. Clinical epigenetics. 2017;9:115.